

Redundancy in active paths of deep networks: a random active path model

Haiping Huang, Alireza Goudarzi, and Taro Toyoizumi
RIKEN Brain Science Institute, Wako-shi, Saitama 351-0198, Japan
(Dated: June 9, 2019)

Deep learning has become a powerful and popular tool for a variety of machine learning tasks. However, it is extremely challenging to understand the mechanism of deep learning from a theoretical perspective. In this work, we study robustness of a deep network in its generalization capability against removal of a certain number of connections between layers. A critical value of this number is observed to separate a robust (redundant) regime from a sensitive regime. This empirical behavior is captured qualitatively by a random active path model, where the path from input to output is randomly and independently constructed. The empirical critical value corresponds to termination of a paramagnetic phase in the random active path model. Furthermore, this model provides us qualitative understandings about dropconnect probability commonly used in the dropconnect algorithm and its relationship with the redundancy phenomenon. In addition, we combine the dropconnect and the random feedback alignment for feedforward and backward pass in a deep network training respectively, and observe fast learning and improved test performance in classifying a benchmark handwritten digits dataset.

Keywords: Neuronal networks, Machine learning, Statistical physics

I. INTRODUCTION

Deep learning (e.g., with many layers of neural networks) works very well in areas from speech recognition, image classification, to drug discovery, medical image analysis, particle discovery, automatic game playing, and many others [1]. This is due to the available large dataset for training and efficient hardware design such as GPU to accelerate training, rather than breakthrough in theoretical foundations. Theoretical efforts are recently devoted to address partially the origin of these amazing performances of deep networks, relying on model assumptions [2–7].

To understand deep learning as a whole is extremely difficult and highly challenging. However, based on simple hypotheses, we are able to provide theoretical insights towards collective properties of deep trained networks, which some regularization techniques used to achieve superior performance. One of them is dropconnect proposed to provide a sampling of model ensemble during training [8], with the purpose to reduce the over-fitting effects, which is common in a fully-connected neural network training, because the number of weight parameters is much larger than the amount of labeled data provided to the deep network. Although dropconnect is quite effective in practice, theoretical justifications or underlying mechanisms are still lacking so far. On the other hand, redundancy in population codes was observed from retina to motor cortex [9–11]. This redundancy emerges from the collective neural code and provides neural mechanism against any possible noise in the neural circuit to maintain its neurophysiological function. In terms of synaptic activities, this kind of redundancy may also appear from interactions between synapses, even during a supervised training of a deep fully-connected feedforward network. The deep architecture should be robust in the absence of a fraction of connections between layers to some extent. In other words, the generalization ability measured by the output error on test data set does not significantly change until a certain amount of connections are removed. Indeed, this is observed in our numerical experiments in this work.

Surprisingly, this typical phenomenon can be qualitatively captured by a simple random active path model, in which we construct randomly and independently each active path from the input at the bottom layer to the output at the top layer, and each path serves as a constraint in a p -weight interaction model (p refers to the depth of the deep network). Increasing the number of path is equivalent to increasing the weight's mean degree in a graphical model representation. The ground state energy of the model decreases with the mean degree until the mean degree grows up to some critical value. This simple theoretical model qualitatively explains why a small dropconnect probability should be avoided for having good generalization ability. In practice, we use the dropconnect probability selected from the redundancy regime, and in a backward pass, a random feedback weight matrix is used to backpropagate the error for saving computation cost. Elements of the random feedback matrix are independently sampled from a uniform distribution with relatively large bound for the support [12]. In particular, the random feedback breaks up the symmetry of connections between layers in a deep network, which is more biologically plausible, since top-down connections may weigh differently the teaching signals generated from high-order brain areas [13, 14].

In particular, the random feedback asymmetry reduces the computer time compared to the standard dropconnect implementation, but still behaves similarly to dropconnect. The current model study adds some qualitative understandings to this scalable algorithm for modern deep learning, and moreover builds connections to physics of p -spin interaction model well studied in physics community [15–18].

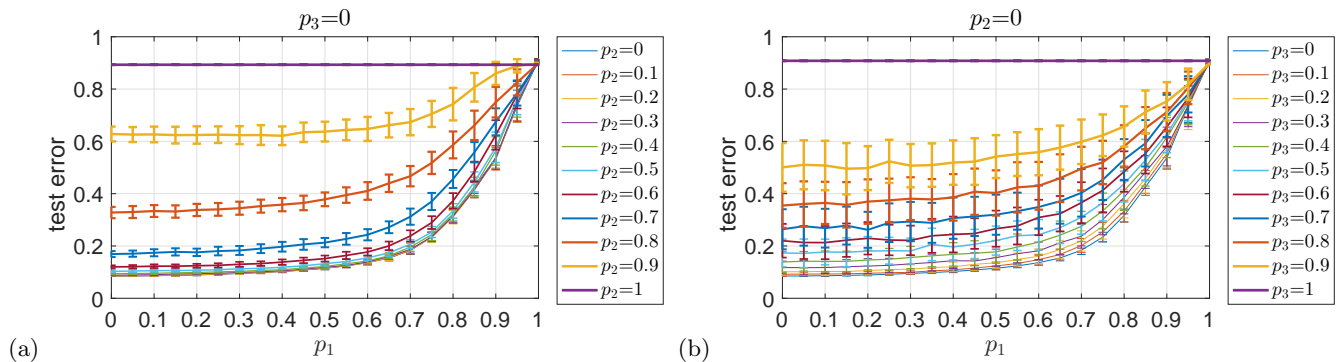


FIG. 1: (Color online) Test error as a function of dilution probability p_l ($l = 1, 2, 3$). (a) p_1 and p_2 vary with constant $p_3 = 0$. (b) p_1 and p_3 vary with constant $p_2 = 0$. We choose training data size $B_1 = 2000$ for training a deep network specified by 784-1000-1000-10, tested on $B_2 = 1000$ validation digits. The total number of epochs is set to 2000, and the initial learning rate is equal to 0.1 divided by 10 every 1000 epochs. The test error is averaged over 100 independent runs.

II. RESULTS

A. Redundancy in active paths of deep networks

We consider a deep network model with L layers of fully-connected feedforward architecture. Each layer has n^l neurons (so-called width of a layer). We define the input as n^0 -dimensional vector \mathbf{v} , and the weight matrix \mathbf{W}^l specifies connections between layer l and layer $l-1$. A bias can also be incorporated into the weight matrix by assuming an additional constant input. The output at the final layer is expressed as:

$$\mathbf{y} = f_L(\mathbf{W}^L f_{L-1}(\mathbf{W}^{L-1} \dots f_2(\mathbf{W}^1 \mathbf{v}))), \quad (1)$$

where $f_l(\cdot)$ is an element-wise sigmoid function for neurons at layer l , defined as $f(x) = \frac{1}{1+e^{-x}}$. Note that for the top layer, we use softmax transfer function as $f_L(a_j) = \frac{e^{a_j}}{\sum_j e^{a_j}}$, where a_j is the weighted sum of inputs into neuron j at the top layer.

The network is trained to learn the labeled handwritten digits on MNIST [19] with B_1 training handwritten digits (from 0 to 9), and after learning, the network is tested on the other different set of B_2 examples. For this supervised learning, we use the cross-entropy defined by $\mathcal{C} = -\sum_{c=1}^{N_c} y_c \ln \hat{y}_c$ as our cost function to minimize, where N_c is the total number of classes, \hat{y}_c is the actual softmax output at the top layer, and y_c is the target label (one-hot representation). The test error characterizes the generalization ability of the learned model. We measure the test error as the classification error defined by $\epsilon_{\text{test}} = \frac{1}{B} \sum_{i=1}^B \mathbb{1}(\hat{y}_i(\mathbf{v}^i) \neq y_i)$, where $\mathbb{1}(\cdot)$ defines an indicator function of an event, and takes value one if the event is true, but zero otherwise. In simulations, we use $L = 4$, thus the deep network architecture is specified by $n^0-n^1-n^2-n^3$. The cross-entropy is minimized by backpropagation of the error from the top layer to the bottom layer.

To visualize the redundancy behavior of active paths, we first introduce a dilution probability p_l , where l specifies the weight population between two consecutive layers (l and $l-1$ -layer). In testing simulations, each weight in a weight population was removed independently with p_l . By varying p_2 with zero p_3 , one can see how the test error changes, as shown in Fig. 1 (a). Interestingly, the test performance is quite robust against increasing p_1 up to some value (e.g., $p_1 \simeq 0.45$). Above this critical value, the test performance deteriorates rapidly with the dilution probability. This property also holds for diluting other weight populations by varying p_2 or p_3 . By varying p_3 with zero p_2 , apart from the same qualitative behavior, we also observe large fluctuations in test error, which deteriorates at a smaller p_3 compared to the critical value of p_2 or p_1 . This indicates that the final layer is more sensitive to network structure perturbation, likely because of its reduced dimensionality in weights compared to that of early layers. Furthermore, we change the width of the second hidden layer, and observe that the typical redundancy behavior does not change significantly in the redundant regime, while the non-redundant regime shows a strong finite-width effect (Fig. 2).

B. A random active path model

In this section, we propose a random active path (RAP) model to understand the redundancy of active paths. An active path refers to the path from one input unit to one output unit with the property that each connection on

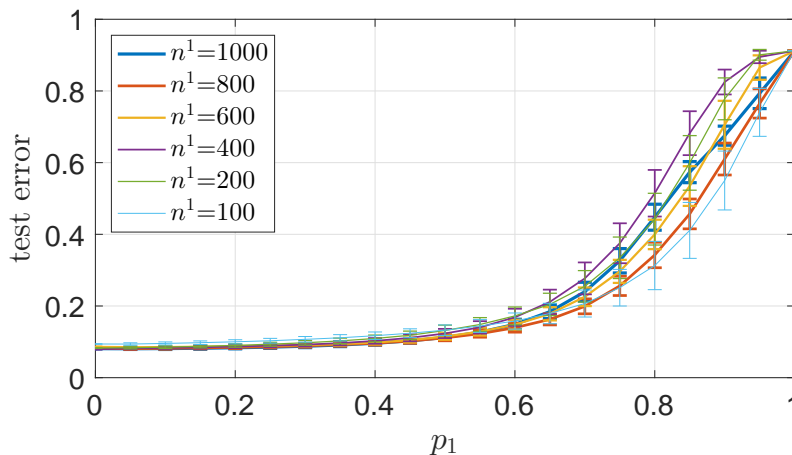


FIG. 2: (Color online) Finite width effect of redundancy of active paths. The deep network is specified by 784- n^1 -1000-10, where n^1 is varied in the plot.

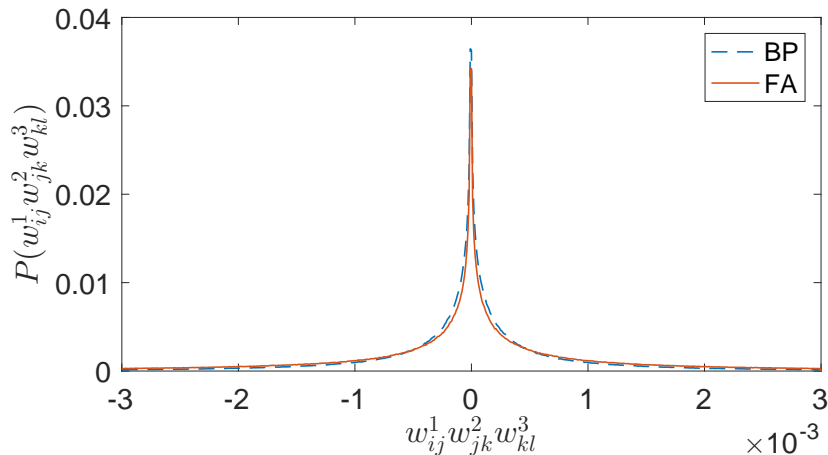


FIG. 3: (Color online) Distribution of weight products in active paths of a deep network trained with either standard backpropagation (BP) or random feedback alignment (FA). The network architecture is specified by 784-100-200-10.

the path is present. We observe that the distribution of products of real-valued weights between consecutive layers (on an arbitrary path) is concentrated around zero, with the property that the product of weights on a chosen path takes negative value or positive value with nearly equal probability (see Fig. 3). Therefore, for L layers, we construct $p = L - 1$ weight populations whose elements take ± 1 with equal probability. The weight population size is fixed to be N , which tends to be infinite in the thermodynamic limit. For simplicity, we assume that the sign of weights is important to constrain the contribution of each path to the global loss of the network [20]. From each population, we randomly pick one weight (say w_i^0) to form an interaction, being $J_a = \prod_{i=1}^p w_i^0$. Each interaction represents a random active path to constrain the weight configuration in a deep network. The above process is repeated for M times, and thus we have the following Hamiltonian for all possible weight configurations in a deep network setting:

$$\mathcal{H}(\mathbf{w}) = - \sum_{a=1}^M J_a \prod_{i \in \partial a} w_i, \quad (2)$$

where ∂a means all the weights involved in the active path a . In fact, Eq. (2) is a disordered p -weight interaction model [15, 17, 18], where here the quenched disorder stems from the random construction process. Clearly, if $\mathbf{w} = \mathbf{w}^0$, the ground state energy is obtained. However, the weight configuration to have a low energy state is not unique in general.

It has been shown that the zero-one loss for a deep non-linear network can be transformed into a p -weight interaction spherical model under a few unrealistic approximations [2], such as activation of any paths is independent of input,

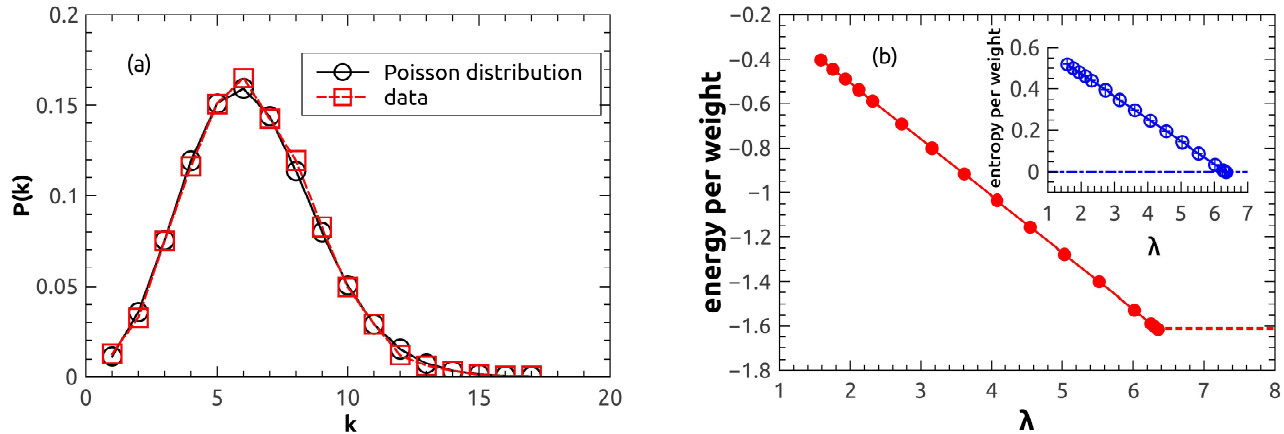


FIG. 4: (Color online) Statistical properties of the RAP model. In simulation, we consider ten random samples of the model with $N = 2000$. (a) The theoretical distribution of weight's degree matches well that obtained from one instance of the model (data). (b) Energy per weight decreases as λ increases, up to some critical value $\lambda_c \simeq 6.336$, from which the energy becomes a constant due to the entropy crisis (the inset).

and all paths have independent inputs. Therefore the energy landscape of p -weight model can be equivalent to the loss surface structure under these coarse-grained settings. Although it is challenging to prove these assumptions reasonable in real deep networks, the p -weight interaction model still provides us a nice starting point to qualitatively understand complicated properties of deep neural networks.

In the current setting, increasing M leads to a high degree of each weight, i.e., each weight is involved in a large number of active paths with high probability. In the thermodynamic limit, one can compute analytically the degree distribution. Here, we consider $p = 3$ (i.e., $L = 4$) for simplicity. It is straightforward to generalize the following formulas to larger p (deeper network). We also assume each layer has equal width \sqrt{N} . First, the probability for an active path is given by $q = \frac{M}{N^2}$. In addition, we have the identity $3M = \tilde{N}\bar{c}$, where \tilde{N} is the total number of weights in Eq. (2), and it is proportional to N with the proportion coefficient α ($\alpha \rightarrow 3$ as $M \rightarrow \infty$), and $\bar{c} = \frac{\sum_{i=1}^{\tilde{N}} d_i}{\tilde{N}}$, where d_i indicates the degree of weight i . Thus $q = \frac{\lambda}{N}$, where $\lambda \equiv \frac{\alpha\bar{c}}{3}$. Now the probability of degree k for an arbitrary weight in Eq. (2) can be written explicitly as follows,

$$P(k) = \lim_{N \rightarrow \infty} \binom{N}{k} q^k (1-q)^{N-k} = \frac{e^{-\lambda} \lambda^k}{k!}, \quad (3)$$

where we have used $\binom{N}{k} \simeq \frac{N^k}{k!}$ in the large N limit. The degree profile is exactly a Poisson distribution with mean degree λ , as also verified by a comparison between the theory and one instance of the model (Fig. 4 (a)).

Similarly, one can prove the relationship between the dilution probability $1 - p_{\text{dc}}$ (e.g., p_1 , p_2 , or p_3) and the mean degree λ , from the fact that $\frac{M}{N^2} = p_{\text{dc}}^3$. It then follows that the dropconnect probability $p_{\text{dc}} = N^{-1/3} \lambda^{1/3}$. Thus for a fixed width, the p_{dc} is proportional to $\lambda^{1/3}$. Tuning p_{dc} amounts to varying λ in the model. Note that for simplicity, we assume here a homogeneous dilution probability for all layers.

The mean-field model defined in Eq. (2) can be solved by the cavity method [21, 22]. The technical details are summarized in methods (Appendix A). As observed in Fig. 4 (b), given the inverse temperature $\beta = 1$, the RAP model has a paramagnetic phase if λ is small, and the energy is decreased rapidly as λ increases, i.e., when the network becomes denser with decreasing dilution probability. At a critical degree, the entropy starts to become negative (so-called entropy crisis), implying that the paramagnetic phase is not thermodynamically dominant any more, and a discontinuous spin phase transition emerges [15, 17, 18]. However, we would not perform a one-step replica symmetry-breaking (1RSB) [15, 18] studies here, and alternatively we adopt a frozen ansatz, i.e., after the critical λ_c , the energy is independent of λ , and fixed according to the zero-entropy condition $S(\lambda_c) = 0$ [23]. In the current model setting, $E_c/\tilde{N} = -1.6115$ at $\lambda_c \simeq 6.336$. The result is shown in Fig. 4 (b). Even though an advanced approximation (e.g., 1RSB) is considered, the energy level is expected to decrease much more slowly in the high degree regime [23]. This behavior mimics the redundancy observed in practical deep network simulations (Fig. 1). Note that this qualitative property does not change when different values of β are considered, with the only difference that energy levels are different at different inverse temperatures.

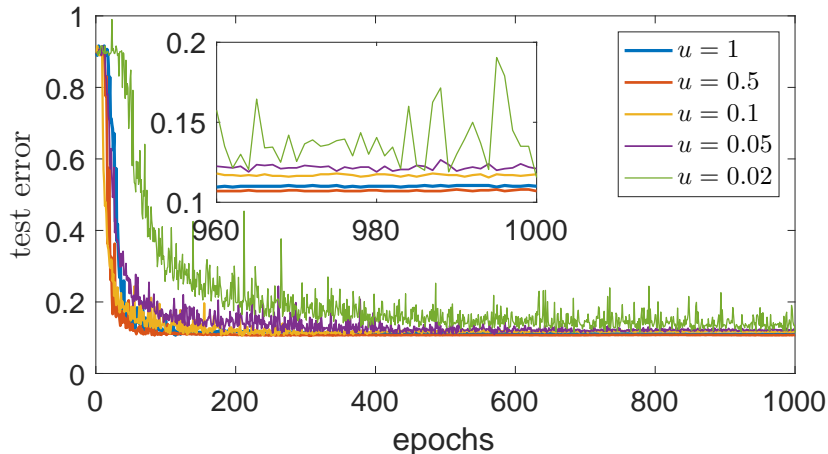


FIG. 5: (Color online) Effects of random feedback-weight-bound u on learning performance. The network architecture is specified by 784-100-200-10, where we apply feedback alignment to the second weight population, and the network is trained on $B_1 = 2000$ examples with the learning rate set to 0.1, and tested on a validation set of $B_2 = 1000$ examples. The inset shows an enlarged view of the later stage.

C. Dropconnect combined with random synaptic feedback improves the test performance

The RAP model provides us qualitative understandings about dropconnect probability and its relationship with redundancy phenomenon. In modern deep network training, one popular regularization technique is called dropconnect, in which during forward pass of the standard backpropagation [24], a binary mask is applied to the feedforward connections, implementing some sort of Bayesian model selection [25]. Entry of the binary mask is set to one with dropconnect probability p_{dc} , and zero otherwise. The redundancy behavior implies that $p_l = 1 - p_{dc}$. Therefore, we can study effects of different values of $1 - p_l$ as the dropconnect probability p_{dc} on the regularization ability of deep networks. Note that small values of p_l maintain the plateau of test error in Fig. 1.

To avoid the computation cost to memorize the dropconnect mask applied in the feedforward pass [8], we use a random feedback weight matrix to propagate the error [12]. Elements of the random feedback weight matrix are independently sampled from a uniform distribution with supports falling within $[-u, u]$, where u denotes the bound of the weight strength. We first test effects of different bounds u on the learning performance by using pure feedback alignment (without dropconnect regularization). The result is shown in Fig. 5, indicating $u = 0.5$ achieves the best performance among all values tested.

As shown in Fig. 6 (a), small values of p_{dc} result in high test error, consistent with the non-redundant regime where the network function is very sensitive to architecture perturbation (i.e., deletion of some connections between layers). In contrast, high values of p_{dc} maintain a good test performance. This is because, as dropconnect is carried out during training, a good model ensemble (robust in performance) is sampled randomly, and the network learning is still able to use the information transmitted from input layer to output layer. As p_{dc} decreases down to some small value, the performance gets worse immediately (Fig. 6 (b)), which is expected from redundancy behavior of active paths in a deep network. Remarkably, this hybrid regularization algorithm improves substantially over the standard backpropagation in the deep network's generalization performance (Fig. 6 (b)). Note that, to make this hybrid regularization algorithm more effective, a small learning rate at the later stage of the training should be used.

III. DISCUSSIONS

In this work, we study the redundancy behavior of network connections on test performance of deep networks. In modern deep learning application, a fully-connected multi-layered neural network is commonly used (or as a part of the network). When a connection between layers is deleted with certain probability, the performance of a trained network is not affected unless this deletion probability increases up to some value, from which the performance starts to get immediately worse. This motivates us to propose a phenomenological model to understand this empirical behavior. We assume the weight products of neighboring layers give constraints on the learning task the network tries to implement. As observed in typical deep network training, these weight products have equal probability to be positive or negative, thus we propose a random active path model, where each path from input to output is

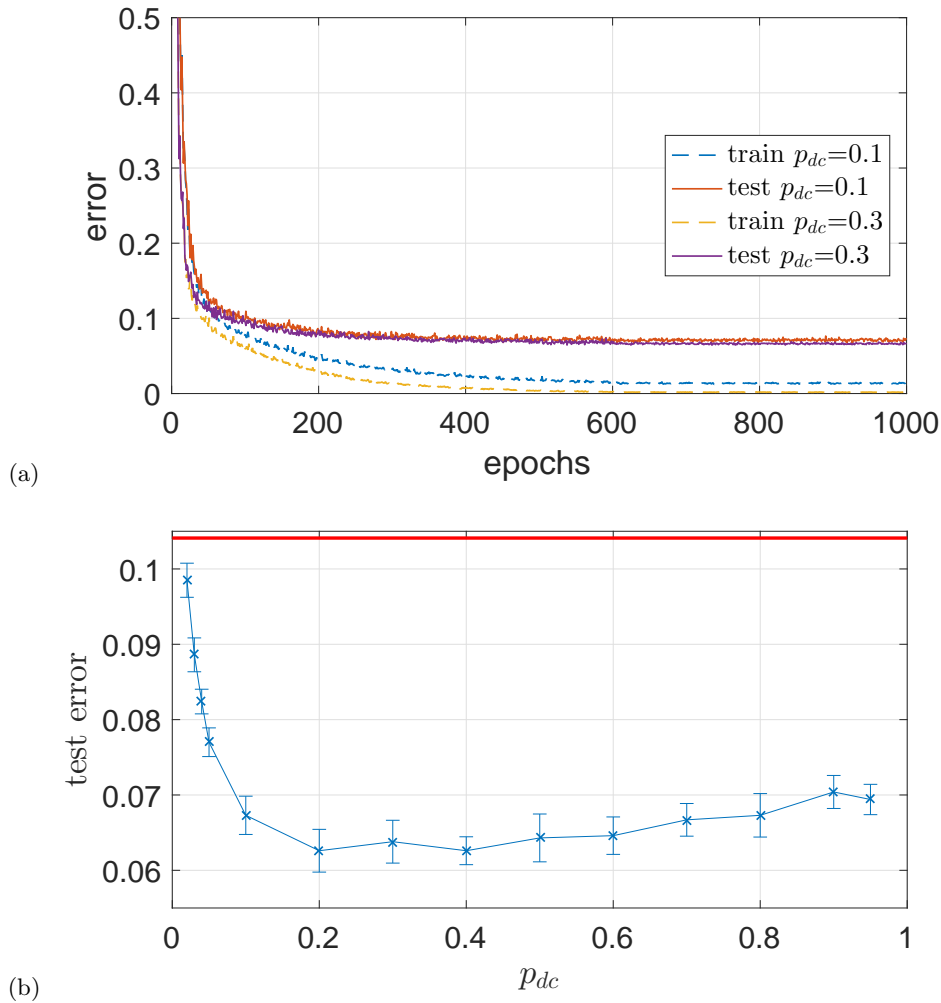


FIG. 6: (Color online) Performance of dropconnect with random feedback alignment. We choose $B_1 = 5000$ for training a deep network specified by 784-100-200-10, with a test set of $B_2 = 2000$ examples. The total number of epochs is set to 1000, and the initial learning rate is equal to 0.1 for the first 600 epochs, 0.005 for the middle 200 epochs, and 0.001 for the final 200 epochs. The feedback weights as well as dropconnect only apply to the connections from layer 3 to layer 2 ($u = 0.5$). During inference of the label of an unseen example, a Gaussian sampling procedure with 100 samples for prediction (model averaging) is used as in Ref. [8]. (a) training dynamics with different dropconnect probability. (b) test error versus dropconnect probability. The test error is averaged over 5 independent runs. The red line shows the result obtained by normal backpropagation.

randomly constructed from pools of weights between consecutive layers. Interestingly, when the number of selected paths increases, the mean degree of each involved weight on a graphical model representation grows as well, which finally leads to disappearance of a paramagnetic phase in the model. The energy in a paramagnetic phase grows as the the graphical model becomes diluted. This thermodynamic behavior mimics the redundancy behavior observed in real deep network training. Given the redundancy property, the deep network has the chance of repairing and modification of subnetworks, without affecting the overall function. It is worth noting that the redundancy property also holds in a deep network where connections are binary (± 1), when the network is trained by stochastic gradient descent with two sets of variables (continuous and corresponding binarized weights) [20].

In addition, by turning on a certain fraction of connections during forward pass of a supervised learning, one can reduce the over-fitting effects of training. This amounts to implementing a model selection, and our phenomenological analysis of a random active path model and redundancy phenomenon offers theoretical insights towards this kind of model selection. When the dropconnect probability is very small, the performance gets worse rapidly as the probability decreases, which is consistent with a rapid increase of the model energy when the mean degree of each weight decreases down to some small value. This suggests that one should choose a relatively large dropconnect probability to implement a sampling of good model ensemble in terms of its robustness in learning performance. The

RAP model explains qualitatively the redundancy behavior, nevertheless, it still needs to be improved by introducing correlations between paths sharing the same input, and thus will have quantitative predictions for deep network training, which deserves further systematic studies.

We also propose a combination of dropconnect with random feedback alignment, to avoid the expensive computation cost of memorizing the dropconnect mask during backpropagating the error. The random feedback matrix breaks the symmetry of connections, with a mechanism closer to biological observations, in the sense that in cortical computation, different weight matrices are used respectively for bottom-up and top-down information processing [13, 14]. We verify that this combination takes effect in classifying handwritten digits on a benchmark dataset MNIST. This hybrid algorithm indeed reduces the over-fitting effects at some optimal values of dropconnect probability, compared to standard backpropagation (Fig. 6 (b)). This efficient combination thus offers the possibility to test its learning capability in much more complicated network architectures and complex dataset.

Appendix A: Mean field method to solve the RAP model

We present self-consistent mean field equations in this appendix to analyze the statistical properties of the RAP model (Eq. (2)). These equations can be derived using the standard cavity method [26], and have been similarly studied in a recent work [22] in a different context. These equations are given by (assuming $\beta = 1$):

$$m_{i \rightarrow a} = \tanh \left(\sum_{b \in \partial i \setminus a} \tanh^{-1} \hat{m}_{b \rightarrow i} \right), \quad (\text{A1a})$$

$$\hat{m}_{b \rightarrow i} = \tanh J_b \prod_{j \in \partial b \setminus i} m_{j \rightarrow b}, \quad (\text{A1b})$$

where $\partial b \setminus i$ denotes the member of interaction b except i , and $\partial i \setminus a$ denotes the interaction set i is involved in with a removed. $m_{i \rightarrow a}$ is interpreted as the message passing from the weight i to the interaction a it participates in, while $\hat{m}_{b \rightarrow i}$ is interpreted as the message passing from the interaction b to its member i . We call this iteration equation the belief propagation, which serves as the message passing algorithm whose fixed point corresponds to the stationary point of the following Bethe free energy [21]

$$F \equiv -\ln Z = -\sum_i \ln Z_i + \sum_a (|\partial a| - 1) \ln Z_a, \quad (\text{A2})$$

where Z is the normalization constant of the model probability $P(\mathbf{w}) \propto e^{-\mathcal{H}(\mathbf{w})}$. The free energy contribution of one weight is given by $Z_i = \sum_{x=\pm 1} \mathcal{H}_i(x)$ and the free energy contribution of one interaction is given by $Z_a = \cosh J_a (1 + \tanh J_a \prod_{i \in \partial a} m_{i \rightarrow a})$. We define the function $\mathcal{H}_i(x) \equiv \prod_{b \in \partial i} \cosh J_b (1 + x \hat{m}_{b \rightarrow i})$. With the free energy, one can estimate both the entropy and the energy of the model which is given by:

$$E = -\sum_i \Delta E_i + \sum_a (|\partial a| - 1) \Delta E_a, \quad (\text{A3a})$$

$$\Delta E_i = \frac{\sum_{x=\pm 1} x \mathcal{G}_i(x)}{\sum_{x=\pm 1} \mathcal{H}_i(x)}, \quad (\text{A3b})$$

$$\Delta E_a = J_a \frac{\tanh J_a + \prod_{i \in \partial a} m_{i \rightarrow a}}{1 + \tanh J_a \prod_{i \in \partial a} m_{i \rightarrow a}}, \quad (\text{A3c})$$

$$\begin{aligned} \mathcal{G}_i(x) = & \sum_{b \in \partial i} \left[J_b \sinh J_b (1 + x \hat{m}_{b \rightarrow i}) + x J_b \cosh J_b (1 - \tanh^2 J_b) \prod_{j \in \partial b \setminus i} m_{j \rightarrow b} \right] \\ & \times \prod_{a \in \partial i \setminus b} \cosh J_a (1 + x \hat{m}_{a \rightarrow i}). \end{aligned} \quad (\text{A3d})$$

The entropy can be obtained by using the standard thermodynamic formula as $S = -F + E$ when $\beta = 1$.

Acknowledgments

This work was supported by the program for Brain Mapping by Integrated Neurotechnologies for Disease Studies (Brain/MINDS) from Japan Agency for Medical Research and development, AMED.

-
- [1] I. Goodfellow, Y. Bengio, and A. Courville, *Deep Learning* (MIT Press, Cambridge, MA, 2016).
 - [2] A. Choromanska, M. Henaff, M. Mathieu, G. Ben Arous, and Y. LeCun, ArXiv e-prints 1412.0233 (2014).
 - [3] P. Chaudhari and S. Soatto, ArXiv e-prints 1511.06485 (2015).
 - [4] K. Kawaguchi, ArXiv e-prints 1605.07110 (2016).
 - [5] D. Soudry and Y. Carmon, ArXiv e-prints 1605.08361 (2016).
 - [6] P. Vardan, Y. Romano, and M. Elad, ArXiv e-prints 1607.08194 (2016).
 - [7] A. B. Patel, T. Nguyen, and R. G. Baraniuk, ArXiv e-prints 1612.01936 (2016).
 - [8] L. Wan, M. Zeiler, S. Zhang, Y. L. Cun, and R. Fergus, in *Proceedings of the 30th International Conference on Machine Learning (ICML-13)*, edited by S. Dasgupta and D. Mcallester (JMLR Workshop and Conference Proceedings, 2013), vol. 28, pp. 1058–1066.
 - [9] J. L. Puchalla, E. Schneidman, R. A. Harris, and M. J. Berry, *Neuron* **46**, 493 (2005).
 - [10] N. S. Narayanan, E. Y. Kimchi, and M. Laubach, *Journal of Neuroscience* **25**, 4207 (2005).
 - [11] E. Schneidman, J. L. Puchalla, R. Segev, R. A. Harris, W. Bialek, and M. J. Berry, *Journal of Neuroscience* **31**, 15732 (2011).
 - [12] Lillicrap Timothy P., Cownden Daniel, Tweed Douglas B., and Akerman Colin J., *Nature Communications* **7**, 13276 (2016).
 - [13] Harris Kenneth D. and Mrsic-Flogel Thomas D., *Nature* **503**, 51 (2013).
 - [14] Harris Kenneth D and Shepherd Gordon M G, *Nat Neurosci* **18**, 170 (2015).
 - [15] E. Gardner, *Nuclear Physics B* **257**, 747 (1985).
 - [16] T. R. Kirkpatrick and D. Thirumalai, *Phys. Rev. B* **36**, 5388 (1987).
 - [17] S. Franz, M. Mézard, F. Ricci-Tersenghi, M. Weigt, and R. Zecchina, *EPL (Europhysics Letters)* **55**, 465 (2001).
 - [18] Montanari, A. and Ricci-Tersenghi, F., *Eur. Phys. J. B* **33**, 339346 (2003).
 - [19] Y. Lecun, L. Bottou, Y. Bengio, and P. Haffner, *Proceedings of the IEEE* **86**, 2278 (1998).
 - [20] M. Courbariaux, Y. Bengio, and J.-P. David, in *Advances in Neural Information Processing Systems 28*, edited by C. Cortes, N. D. Lawrence, D. D. Lee, M. Sugiyama, and R. Garnett (Curran Associates, Inc., 2015), pp. 3105–3113.
 - [21] M. Mézard and G. Parisi, *Eur. Phys. J. B* **20**, 217 (2001).
 - [22] H. Huang, *Journal of Statistical Mechanics: Theory and Experiment* **2017**, 033501 (2017).
 - [23] T. Nakajima and K. Hukushima, *Phys. Rev. E* **80**, 011103 (2009).
 - [24] Rumelhart David E., Hinton Geoffrey E., and Williams Ronald J., *Nature* **323**, 533536 (1986).
 - [25] H. Huang, ArXiv e-prints 1703.07943 (2017).
 - [26] M. Mézard and A. Montanari, *Information, Physics, and Computation* (Oxford University Press, Oxford, 2009).